Journal of Hydrology: Regional Studies 27 (2020) 100655

Contents lists available at ScienceDirect

Journal of Hydrology: Regional Studies

journal homepage: www.elsevier.com/locate/ejrh

Conceptual hydrological model calibration using multi-objective optimization techniques over the transboundary Komadugu-Yobe basin, Lake Chad Area, West Africa

O.E. Adeyeri[a,b,*], P. Laux[b,d], J. Arnault[b], A.E. Lawin[c], H. Kunstmann[b,d]

[a] West African Science Service Centre on Climate Change and Adapted Land Use, University of Abomey-Calavi, Benin
[b] Institute for Meteorology and Climate Research Atmospheric Environmental Research, Karlsruhe Institute of Technology, Campus Alpine, Germany
[c] Laboratory of Applied Hydrology, National Water Institute, University of Abomey-Calavi, Benin
[d] University of Augsburg, Institute of Geography, Augsburg, Germany

ARTICLE INFO

Keywords:
Optimization techniques
Wavelet analysis
Base flow
High flow
GR5J
Lake Chad

ABSTRACT

Study Area: The discharge of the transboundary Komadugu-Yobe Basin, Lake Chad Area, West Africa is calibrated using multi-objective optimization techniques.
Study focus: The GR5J hydrological model parameters are calibrated using six optimization methods i.e. Local Optimization-Multi Start (LOMS), the Differential Evolution (DE), the Multi-objective Particle the Swarm Optimization (MPSO), the Memetic Algorithm with Local Search Chains (MALS), the Shuffled Complex Evolution-Rosenbrock's function (SCE-R), and the Bayesian Markov Chain Monte Carlo (MCMC) approach. Three combined objective functions i.e. Root Mean Square Error, Nash- Sutcliffe efficiency, Kling-Gupta efficiency are applied. The calibration process is divided into two separate episodes (1974–2000 and 1980–1995) so as to ascertain the robustness of the calibration approaches. Runoff simulation results are analysed with a time-frequency wavelet transform.
New hydrological insights for the region: For calibration and validation stages, all optimization methods simulate the base flow and high flow spells with a satisfactory level of accuracy. For calibration period, MCMC underestimate it by -0.07 mm/day. The performance evaluation shows that MCMC has the highest values of mean absolute error (0.28) and mean square error (0.40) while LOMS and MCMC record a low volumetric efficiency of 0.56. In all cases, the DE and the SCE-R methods perform better than others. The combination of multi-objective functions and multi-optimization techniques improve the model's parameters stability and the algorithms' optimization to represent the runoff in the basin.

1. Introduction

Hydrological modelling is vital for effective water resources management (Bellin et al., 2016). The goal of a hydrological model is to accurately represent the hydrological systems in order to evaluate the impact assessment and risk evaluation related to water resources management in a river basin (Donelly-Makowecki and Moore, 1999). This involves the simplification of the real-world system by means of mathematical equations and assumptions concurrently with input and forcing data, model parameters, and their initial values (Gupta et al., 1998).

* Corresponding author at: West African Science Service Centre on Climate Change and Adapted Land Use, University of Abomey-Calavi, Benin.
E-mail address: cyndyfem@gmail.com (O.E. Adeyeri).

https://doi.org/10.1016/j.ejrh.2019.100655
Received 13 July 2019; Received in revised form 2 December 2019; Accepted 3 December 2019
Available online 12 December 2019
2214-5818/ © 2019 The Authors. Published by Elsevier B.V. This is an open access article under the CC BY-NC-ND license (http://creativecommons.org/licenses/BY-NC-ND/4.0/).

Each hydrological model has its constraints in terms of the number of input data, spatial variability representation, calibration parameters and duration. In particular, some hydrological models have been developed to represent a simplified representation, relationship and transformation of precipitation into runoff (Singh and Woolhiser., 2002; Narasayya et al., 2013). These so-called rainfall-runoff models are created to characterize the physical components of a basin by assuming a simplified rainfall-runoff relationship; without explicit representation of the spatial variability in topography, vegetation and soil properties. The advantage of these models is that they require fewer input data. Additionally, they are simpler to set up and have fewer calibration parameters. As a consequence, they are widely used for operational applications (Lampert and Wu, 2015; Narasayya et al., 2013) as well as for investigating the future changes in climate and land use (Beven, 2011). In this type of model, the parameters selection is restricted to a predefined range in order to achieve a realistic representation of the basin properties (Sorooshian and Gupta, 1995). Furthermore, these parameters are indirectly estimated using calibration and optimization procedures (Gupta et al., 1998). The best model parameter sets during the calibration procedures are benchmarked on objective functions which indicate the degree of numerical agreement between basin observations and model simulations.

Previous researches (e.g. Lu et al., 2013; Duan, 2003) illustrate that calibrations based on a single-objective function are effective for emphasizing a definite characteristic of a system, however, causing increasing errors in other characteristics of the system (Wagener, 2003). In hydrological simulations, for instance, a calibration based on an objective function fine-tunes the model simulation in favour of the predetermined objective function which does not assure a better simulation with other objective function. A multi-objective calibration method seeks to address this limitation by quantifying the adjustments in maximizing or minimizing a number of objective functions, finding a representative set of the Pareto optimal solutions, as well as defining a single solution that maximizes or minimizes a specific independent preference (Gupta et al., 2009; Van Werkhoven et al., 2009).

According to Yapo et al. (1998), multi-objective calibrations are of great advantage as it ensures desired outcomes in hydrological applications. A detailed report of the advantages of this technique is summarized in Efstratiadis and Koutsoyiannis (2010). Thenceforth, many hydrological studies have applied this technique by weighing various objective functions (Foglia et al., 2009; Li et al., 2010), population-based search method, and Pareto set search (Bekele and Nicklow, 2007; Dumedah et al., 2010). In similar attempts, Rakovec et al. (2016) calibrated the mesoscale Hydrologic Model (mHM) (Kumar et al., 2013) over 83 European basins using the Multi-scale Parameter Regionalization approach for improved physiographic and hydrologic regimes. Ning et al. (2015) calibrated the Hydrological Predictions for the Environment model (Lindstrom et al., 2010) over the Da River Basin of Vietnam using the Differential Evolution Markov Chain Monte Carlo (Braak, 2006) step-wise calibration method. Werth et al. (2009) applied the multi-objective calibration framework of Non-Dominated-Sorting-Genetic-Algorithm-II (Deb et al., 2002, NSGAII) to calibrate the WaterGAP Global Hydrology Model (Doll et al., 2003) over the Congo basin in Africa, the Amazon basin in South America, and the Mississippi basin of North America. Xie et al. (2012) calibrated the Soil and Water Assessment Tool model (Arnold and Fohrer, 2005) using the NSGAII technique to assess the total water storage variability over Sub-Saharan Africa basins.

While previous studies established the advantages of using multiple-objective functions over a single criterion, they do not consider the effect of using combined multi-optimization procedures and multiple-objective functions on model parameters set. The advantage of using various optimization methods lies in its ability to assess quality phases of the optimized solutions such as their accuracies, diversities and cardinalities (Riquelme et al., 2015).

In order to reduce the errors being propagated by the use of single objective function as well as generating good optimized solutions for the model parameter sets, this study attempts to calibrate a 5-parameter daily lumped rainfall-runoff model i.e. *le modèle du Génie Rural à 5 paramètres au pas de temps Journalier* (GR5J) (Coron et al., 2017) over the Komadugu-Yobe Basin (KYB) in West Africa using a combined multi-optimization procedures and multiple-objective functions. A detailed description of the study area is given in Section 2. The GR5J model, the calibration and optimization methods are presented in Section 3. Results are provided in Section 4, followed by a summary and conclusion in Section 5.

2. Study area and data

The KYB is a transboundary basin shared by Niger Republic and Nigeria and has area coverage of 150,000 km^2 (Fig. 1). It is a sub-basin of the larger Lake Chad basin. It is predominantly dominated by scattered trees, dense grass and shrubs (Adeyeri et al., 2017). The recurrent migration of the Inter-Tropical Convergence Zone (ITCZ) creates highly seasonal rainfall accustomed by very strong convective storms. The rainy season is between May and October (Thompson and Polet, 2000). The maximum temperature varies between 27 °C in the southern part and 35 °C in the northern part of the basin while the mean annual rainfall varies between 240 mm in the northern part and 1060 mm in the southern part (Adeyeri et al., 2017). The annual potential evaporation varies between 1800 mm and 2400 mm while the evaporation rate is 203 mm per annum (Adeyeri et al., 2019a). The basin is principally drained by the Komadugu Yobe and the Komadugu Gana river sub-systems. August is the wettest month while annual flow ends in late September. The KYB is strategic because its wetlands are sources to some internationally shared waters which are important for both national and international economy.

The climate data used for driving the GR5J, namely precipitation and temperature is provided by Direction de la Meteorologie Nationale (DMN) of the Niger Republic and Nigeria Meteorological Agency (NiMet) archived at daily time steps. Outliers and negative rainfall values are corrected with a quality control procedure. Homogeneity checking and correction is done using a multi-break method based Adapted Caussinus-Mestre Algorithm for homogenising Networks of Temperature series (ACMANT). A comprehensive report on ACMANT set up can be found in Domonkos and Coll (2017). Results from previous studies (e.g. Domonkos and Coll, 2017; Barbara et al., 2018; Adeyeri et al., 2019b) show that ACMANT performs well in homogenising climate variables (rainfall, relative humidity and temperature). The potential evapotranspiration is calculated using Oudin et al. (2005) approach. The daily

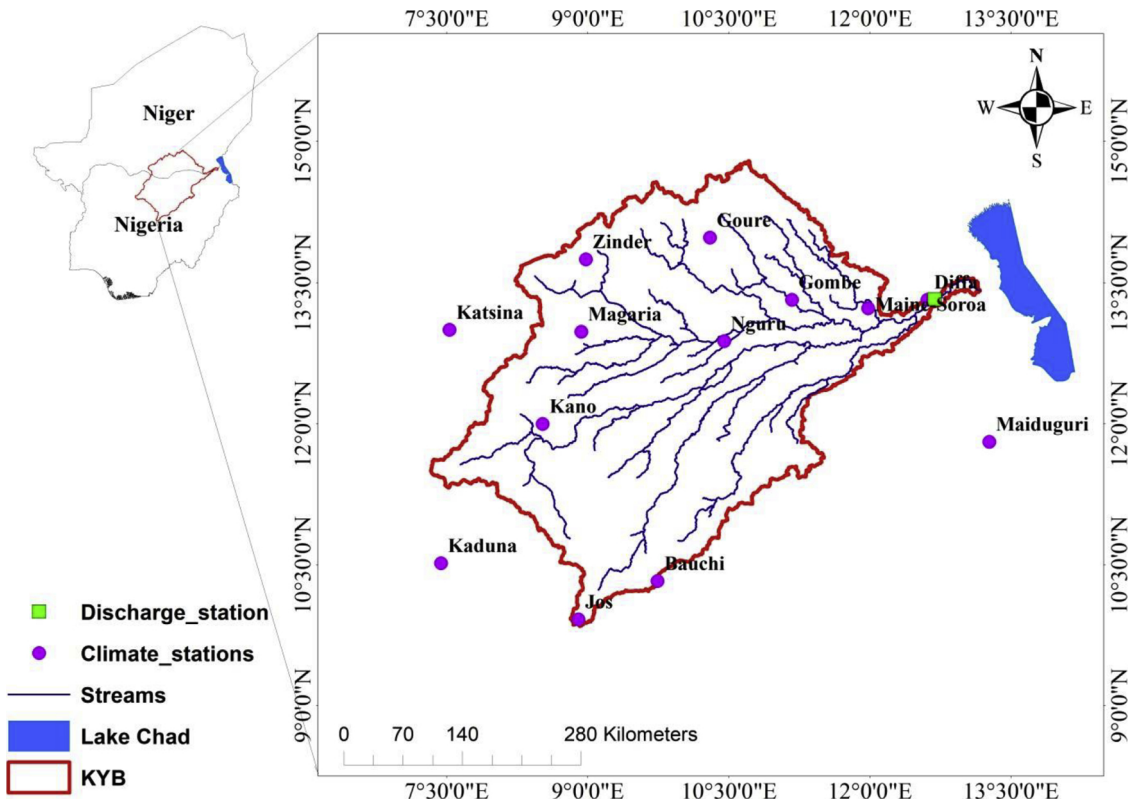

Fig. 1. Study Area.

runoff data is provided by the Diffa hydrological station. The analysis period is between 1971 and 2013.

3. Hydrological model, calibration and optimization methods

In this section, the GR5J model, as well as the multi-objective and the multi-optimization methods are described. The schematic of the methodology is presented in Fig. 2

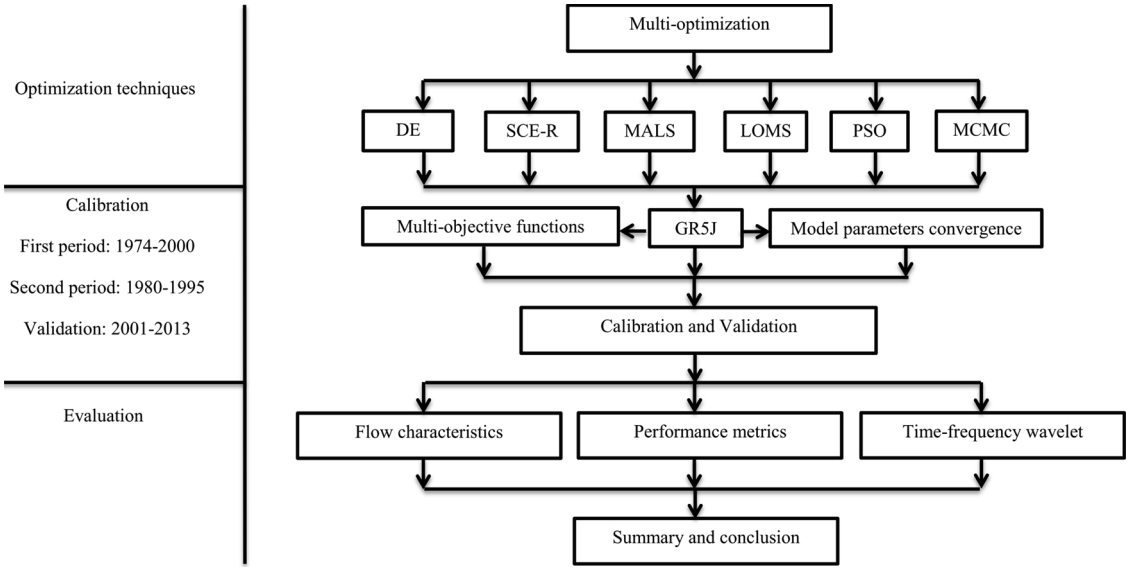

Fig. 2. Methodology flow chart.

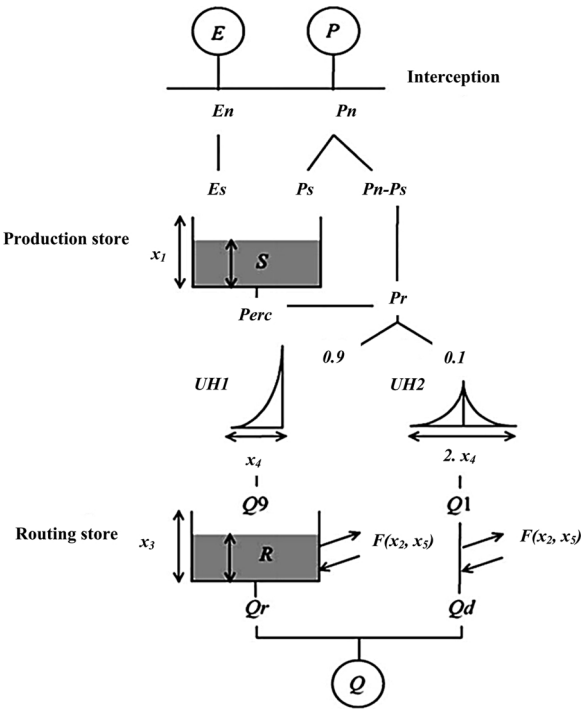

Fig. 3. GR5J model set up (from: Lavenne et al., 2016; Mostafaie et al., 2018).
P is the areal basin rainfall, E is the mean of inter-annual potential evapotranspiration, Pn is the net rainfall, En is the net evapotranspiration, S is the production store, Perc is percolation amount, R is the routing store, Q9 and Q1 are the outputs of the unit hydrographs UH1 and UH2 respectively, Q is the total runoff.

3.1. The GR5J model

The GR5J model (Le Moine, 2008; Lavenne et al., 2016) is a rainfall-runoff model that focuses on soil moisture partition. The general model structure is presented in Fig. 3. Five model parameters can be calibrated, namely the maximum capacity production store, X1 (mm) and a maximum capacity routing store, X3 (mm) which are the two store compartments fed by the time base of a unit hydrograph, X4 (days). The two other parameters, i.e. the inter-catchment exchange coefficient, X2 (mm/d) and the inter-catchment exchange threshold, X5, which quantifies the inter-catchment groundwater flows. X1 and X2 are connected to water balance (Table 1). The degree-day snow module (Valéry et al., 2014) is not activated in this study, as there is no snow in our application study. X1 and X3 are positive real numbers, X2 accepts both positive and negative numbers while X4 is always greater than 0.5 (Perrin et al., 2003). The inputs for the model are precipitation and evapotranspiration. Additionally, the ordinary krigging method (Li and Heap, 2014) is used to calculate the area mean basin rainfall.

3.2. Multi-objective calibration

Multi-Objective model calibration is based on objective functions suitable for various hydrological processes such as peak flows, general and low flows (Madsen, 2000). This reduces the errors being propagated by the use of a single objective function.

A multi-objective calibration problem can be expressed as:

$$\min[F_1(\varnothing), F_2(\varnothing), \ldots, F_m(\varnothing)], \ \varnothing \in \ominus \quad (1)$$

Where, $F_m(\varnothing)$ are the different objective functions.

Table 1
Model parameters.

Parameters	Meaning	Unit
X1	production store capacity	mm
X2	Inter-catchment exchange coefficient	mm/day
X3	Routing store capacity	mm
X4	Unit hydrograph time constant	day
X5	Inter-catchment exchange threshold	–

∅ is the model parameters while ⊖ is the parameter space. The model parameters are restricted to physically plausible parameter space. The upper and lower bounds of the model parameters are specified as a hypercube function of the parameter space. Eq. (1) reaches a Pareto set of solutions given an optimal trade-off among the different objective functions (Gupta et al., 2003).

The multi-objective method selected for this study consists minimizing the root mean square error and maximizing both, the Nash-Sutcliffe and the Kling-Gupta efficiencies. The Root Mean Square Error (RMSE) is a commonly used statistic that provides a good overall measure of how close modelled values are to predicted values.

$$\mathrm{RMSE}= \sqrt[2]{\frac{\sum_{i=1}^{n}(M_i - O_i)^2}{n}} \tag{2}$$

where, O_i represents the ith observed value and M_i represents the ith model value for a total of n observations. The Nash and Sutcliffe Efficiency (NSE) compares the relative magnitude of the residual variance to observation variance (Nash and Sutcliffe, 1970).

$$\mathrm{NSE}= \frac{\sum_{i=1}^{n}(Q_o - Q_{av})^2 - \sum_{i=1}^{n}(Q_o - Q_s)^2}{\sum_{i=1}^{n}(Q_o - Q_{av})^2} \tag{3}$$

Q_o is the observed discharge, Q_{av} is the average observed discharge, Q_s is the simulated discharge. NSE varies between -∞ and 1 with the optimum value being 1. However, due to the quadratic nature of NSE, it provides information on the model's ability to simulate high flows. NSE can also return optimum values as a result of periodicity, thereby providing a misleading interpretation of the model's ability. As a result of these lapses, many studies (e.g. Mathevet et al., 2006; Criss and Winston, 2008) decomposed the NSE into a ratio of standard deviations (αNSE), relative bias (βNSE) and the ratio of the correlation coefficient (r). Gupta et al. (2009) showed that optimizing αNSE underestimates the variability of simulated flows because the optimum NSE is attained when αNSE = r. In view of this, Gupta et al. (2009) and Kling et al. (2012) recommended the Kling-Gupta efficiency (KGE) in order to circumvent the connections between the variation coefficient and bias and ratios.

$$\mathrm{KGE}= 1 - \sqrt{(\mathrm{rc}-1)^2 + (\beta_{\mathrm{KGE}} - 1)^2 + (\gamma_{\mathrm{KGE}} - 1)^2} \tag{4}$$

where, rc is the linear Pearson correlation coefficient, β_{KGE} is the bias and γ_{KGE} is the variation coefficient ratio.

3.3. Multi-optimization methods

In this study, six different multi-optimization methods are used for the calibration of the model parameters. The results of the multi-optimization technique provide a set of solutions which concurrently optimize conflicting objective functions in a population set, leading to a Pareto-optimal solution of the model parameters (Savic, 2002). The six methods are briefly explained in the following.

3.3.1. Particle swarm optimization (PSO)

The PSO is a population-based stochastic global optimization procedure (Kennedy and Eberhart, 1995). In this method, the population of potential solutions is called a swarm while particles are the members of the swarm. These particles change positions in a multi-dimensional search space depending on the position of other particles in the swarm as well as their own relative positioning. The process involves the adjustment of the system based on a set of arbitrary solutions while the optimization search is maintained as the generations are updated. The history of the best positions of the particles is retained by the neighbouring particles while considering their fitness level after each iteration. This helps in refining the final solution. The process reaches finest optimization when all particles converge. The advantages of this method include its ability to converge fast, high efficiency in finding global optimal and its ability to run parallel computation. The disadvantages include its ability to converge prematurely and subsequently be stuck into a local minimum. Further details can be found in Clerc and Kennedy (2002). While this method has been widely used in fields like neuro-computing and some environmental science field, it is scarcely used in hydrology.

3.3.2. Shuffled complex evolution with Rosenbrock's function (SCE-R)

The advantage of this method lies in its ability to combine both local and global optimization techniques. It starts with a direct local search (Rosenbrock 1960). When the value of the objective function is decreasing, the length of the search vector is increased in order to have an optimum solution. The iteration stops when the initial parameter setting is retained, a new minimum is reached or all axes are explored. The global search combines the shuffling of complexes i.e. partitioning the sample points from a population into distinct groups, competitive evolution and controlled random search with simplex search (Duan et al., 1992, 1993). These enhance information sharing about the search space created individually by each complex. However, iteration takes time on instances of many parameters while trying to maintain a satisfactory level of diversity. This method has been used widely to locate the global optimum for rainfall-runoff models (Cooper et al., 2007; Goswami and Kieran, 2007).

3.3.3. Memetic Algorithms with local search chains (MALS)

MALS is a steady-state memetic algorithm with improved genetic algorithms per local search techniques (Molina et al., 2010). They are particularly suitable for uninterrupted optimization, as they combine the strength of evolutionary algorithms with a local search routine to find the local optimum of a likely region i.e. it combines both local and global optimization techniques. The local search intensity is increased to get the most likely solution. In MALS, the worst solution is substituted in the population instead of

substituting every individual after iterations. This retains the improvement of the solution after the local search (Bergmeir et al., 2016) and subsequently controls the local search procedure to the most likely solutions. However, this method does not perform well if the numbers of parameters to optimize are many.

3.3.4. Differential evolution (DE)

DE is based on a global population stochastic search procedure suitable to find the global optimum in a continuous search domain (Storn and Price, 1997). DE does not require derivatives of the objective function. In DE procedure, a good optimized solution requires a trial-and-error search to adjust its related parameter values. This method is useful in conditions where the objective functions are difficult to differentiate. However, DE is inefficient on smooth functions which are mostly derivative based. This method has been successfully applied for pattern recognition (Ilonen et al., 2003), communications (Storn, 1996) and engineering (Joshi and Sanderson, 1999). Details of this method are presented in Qin et al. (2010).

3.3.5. Bayesian Markov Chain Monte Carlo simulation (MCMC)

This method uses an adaptive metropolis algorithm and a delayed rejection procedure in implementing a Markov Chain Monte Carlo simulation. MCMC aims to generate parameter values' samples by simulating random processes having the posterior distribution as stationary distribution. This posterior distribution is the probability distribution on the parameter space. MCMC further explores the posterior distribution by creating random processes with stationary distribution as the parameters' posterior distribution. The new parameters in the adaptive metropolis are created with a covariance matrix which adjusts to the size and shape of the object distribution. This permits a more proficient posterior distribution exploration. The new parameters generated during delayed rejection are from the scaled covariance matrix jump arising from the last accepted value. This preserves the reversibility of the Markov chain. Advantages of the MCMC include its computational and statistical efficiency. Additionally, tuning the scheme does not require trial runs. However, scaling is poor when there is an infinite target distribution variance. This is not revealed during the inspection of the target density which makes it difficult to detect analytically. Furthermore, it takes time for MCMC to recover from distorted preliminary information because it adapts too closely to the preliminary information from the output. Details are documented in (Haario et al., 2005, 2006).

3.3.6. Local optimization-multi start approach (LOMS)

The Local Optimization-Multi Start approach (LOMS) is a simple bounded and box-constrained general optimization technique (Gay, 1990). In LOMS, the performance of optimization is affected by scale vector chosen in computing the sample's trial values and in testing the convergence of parameters. This strategy requires setting up the start point in transformed parameter space. However, the multi-start approach assesses the consistency in the local optimization method. The downside of this method is that it is bounded by the value ranges of the initial parameters. The details of this method are documented in Gay (1990).

3.4. Modelling strategy

To ascertain the robustness of the optimization techniques, calibration methods and model output, the analysis period is divided into two episodes (Table 2). This provides worthwhile information on the model's ability to replicate the runoff at different times. The calibration period for episode 1 is between 1974 and 2000 and the validation period is between 2001 and 2013 while episode 2 has the calibration period between 1980 and 1995 and the validation period is between 1996 and 2011. In calibrating the GR5J model, the initial model parameters are fine-tuned with a set of trial-and-error experiments before the start of the optimization objectives. In the modelling set up, each optimization technique is run separately in the hydrological model using the multi-objective calibration technique for each calibration and validation periods. The number of iteration and simulation needed for each model parameter to converge for each optimization method is reported. Furthermore, the properties of the runoff generated with each optimization techniques are analysed and compared with the observation.

3.5. Time-frequency wavelet

The transient behaviour of the runoff is examined with time-frequency wavelet analysis. The wavelet transform decomposes signals in a way in which the signal trends and details are represented as a function of time. This shows areas with high common power in the time-frequency space i.e., a transient and localized behaviour at different time scales. The wavelet power spectrum of the runoff local covariance across different time scales is generated based on the wavelet energy stress of the time series (Veleda et al., 2012; Adeyeri et al., 2019a). The advantage of this transformation lies in its ability to deconstruct complex signals into basic signals of finite bandwidth without a phase-shifting or signal leakage of the primary signal.

Table 2
Analysis period.

Episode	Warm up period	Calibration period	Validation period
1	1971–1973	1974–2000	2001–2013
2	1974–1979	1980–1995	1996–2011

Table 3
Statistics of the multi-objective calibration approaches.

	Episode 1(1974–2000)		Episode 2(1980–1995)	
Strategy	Iterations	Simulations	Iterations	Simulations
SCE-R	41	629	52	745
DE	200	402	200	402
PSO	113	4520	110	4400
MALS	2248	2747	2320	2675
LOMS	75	420	69	451
MCMC	40	2992	56	2986

3.6. Numerical performance metrics

The numerical performance metrics used for evaluation of the entire calibration and validation periods are the mean absolute error (MAE), the mean square error (MSE), the normalized root mean square error (NRMSE), the percentage of bias (PBIAS) (Yapo et al., 1996), the ratio of root mean square error to the standard deviation (RSR) (Moriasi et al., 2007), the index of agreement (d) (Legates and McCabe, 1999) and the volumetric efficiency (VE) (Criss and Winston, 2008).

4. Results and discussion

In this section, the results of the multi-objective optimization approaches are described. Further results include the model parameters convergence, flow characteristics, performance metrics as well as the wavelet decomposition of the simulated runoff.

4.1. Multi-objective optimization calibration

The summary of the multi-objective optimization computation is presented in Table 3. It is observed that the global optimization approach of MALS exhibits the highest number of iterations while the PSO has the highest number of simulations for both calibration episodes. This agrees with Sahoo et al. (2010) who emphasised that global optimisation techniques require more computing resources. The lowest iterations and simulations are exhibited by the SCE-R approach in all cases (Seong et al., 2015). The optimum model parameters generated during calibration for each optimization method (Table 4) is used in running the model during validation for the two episodes.

The result for the first episode shows that SCE-R, DE, PSO and MALS methods have the NSE, KGE and RMSE of 0.89, 0.81 and 0.24 respectively for the calibration period (1974–2000) while the validation period (2001–2013) seem to be an improvement over the calibration period. The NSE, KGE and RMSE generated during this period are 0.91, 0.84 and 0.23 respectively. The correlation plot for the calibration period (1974–2000) for the first episode (Fig. 4a) shows the simulated runoff generated by PSO optimization method has the highest correlation with the observed runoff (QOBS) with a value of 0.79. However, there is a degree of correlation

Table 4
Multi-objective sets of calibration parameters during the calibration and validation periods for the two analysis epochs.

Episode 1											
	Calibration Best Parameters					Calibration (1974–2000)			Validation (2001–2013)		
Strategy	X1 (mm)	X2 (mm)	X3 (mm)	X4 (day)	X5	NSE	KGE	RMSE	NSE	KGE	RMSE
SCE-R	100.25	−14.96	1000.52	20	0.40	0.89	0.81	0.24	0.91	0.84	0.23
DE	100.25	−14.96	998.68	20	0.40	0.89	0.81	0.24	0.91	0.84	0.23
PSO	100.25	−14.98	999.18	20	0.40	0.89	0.81	0.24	0.91	0.84	0.23
MALS	100.25	−14.96	998.68	20	0.40	0.89	0.81	0.24	0.91	0.84	0.23
LOMS	800.83	−14.77	200.35	30	0.09	0.67	0.72	0.65	0.74	0.74	0.61
MCMC	800.95	−14.25	200.35	30	0.08	0.67	0.72	0.65	0.74	0.74	0.61
Episode 2											
	Calibration Best Parameters					Calibration (1980–1995)			Validation (1996–2011)		
SCE-R	101.78	−14.98	1000.52	20	0.40	0.89	0.79	0.23	0.92	0.84	0.21
DE	101.78	−14.95	1000.14	20	0.40	0.89	0.79	0.23	0.92	0.84	0.21
PSO	101.98	−14.96	1000.18	20	0.40	0.89	0.79	0.23	0.92	0.84	0.21
MALS	100.25	−14.95	1000.14	20	0.40	0.89	0.79	0.23	0.92	0.84	0.21
LOMS	800.46	−10.95	200.35	30	0.44	0.71	0.69	0.66	0.73	0.73	0.53
MCMC	800.95	−10.11	200.35	30	0.44	0.71	0.69	0.66	0.73	0.73	0.53

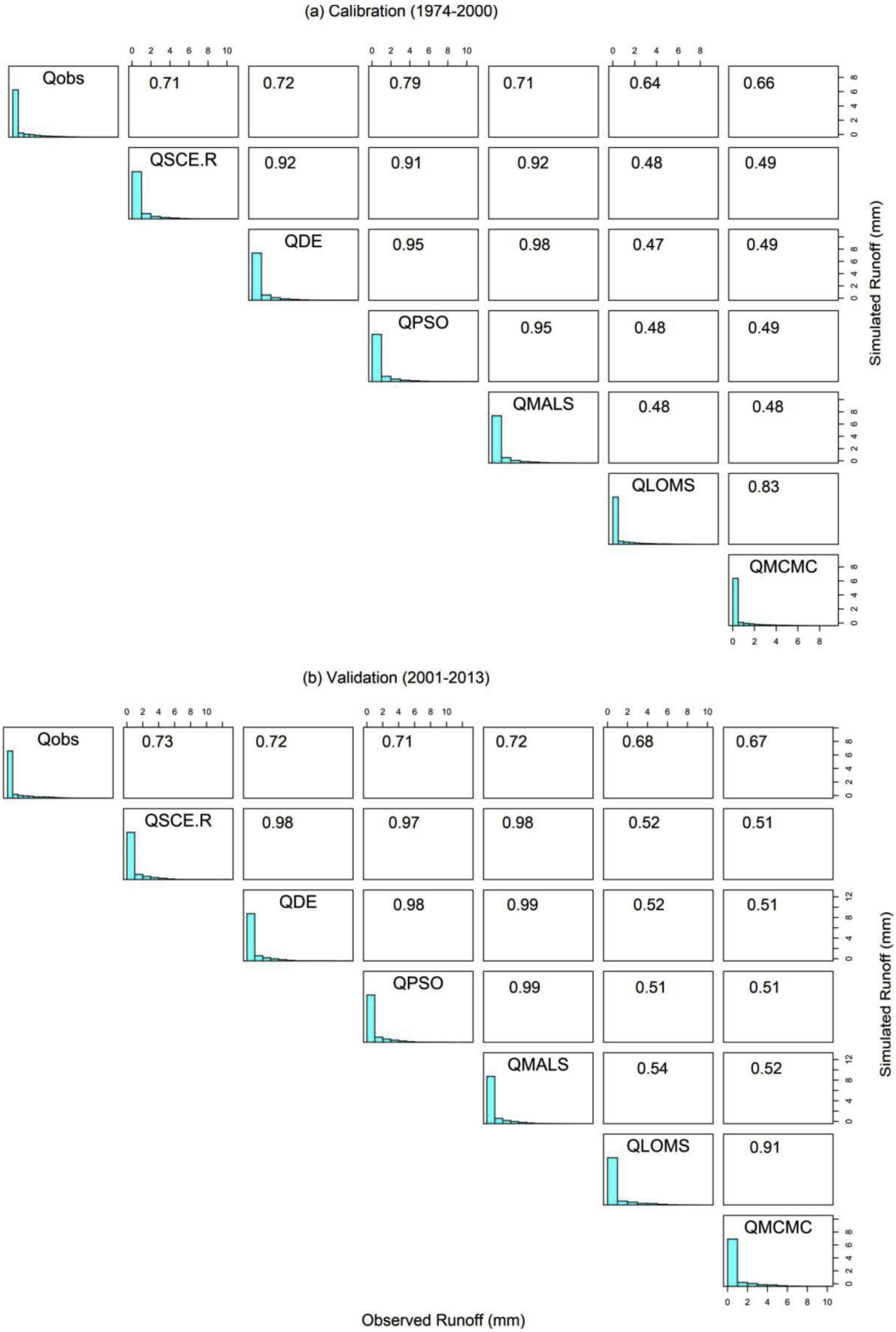

Fig. 4. Correlation plot for the (a) calibration period (1974–2000) (b) validation period (2001–2013).

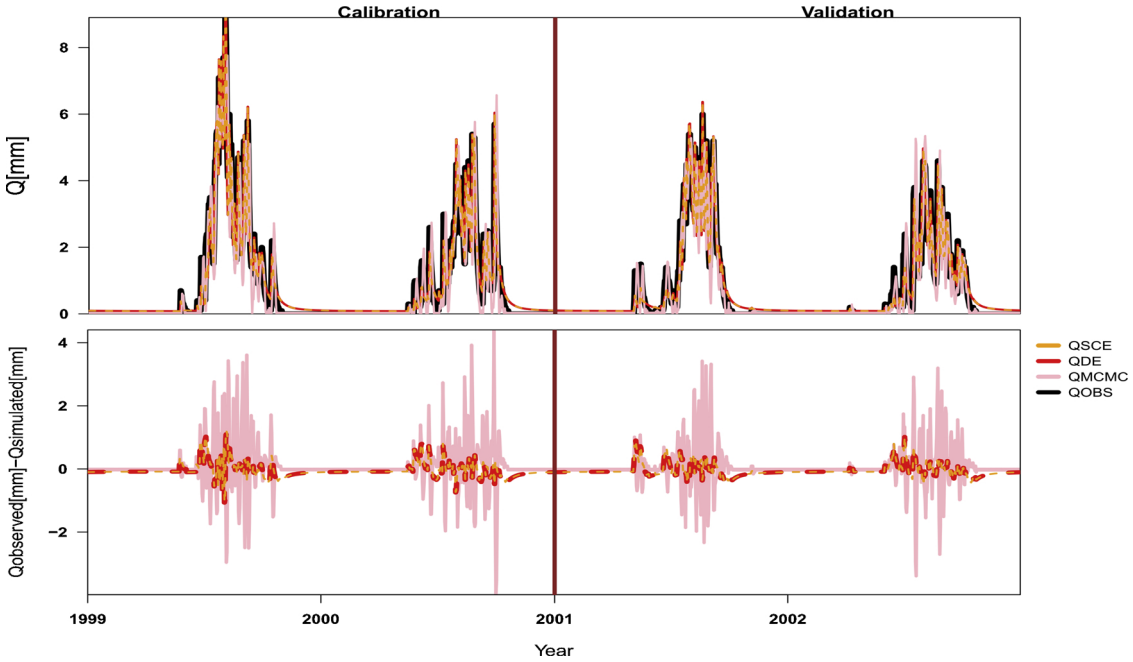

Fig. 5. Above: Comparison of daily observed runoff with GR5J-simulated runoff using different optimization methods. Below: GR5J-simulated runoff anomaly with observation for sub-calibration period (1999–2000) and sub-validation period (2001–2002). Q is daily runoff.

between simulated runoff generated by all optimization algorithms. The correlation plot for the validation period (2001–2013) shows a high degree of correlation between the observed runoff and the simulated runoff from SCE-R, DE, PSO and MALS optimization methods (Fig. 4b). Nevertheless, SCE-R optimization method has the highest correlation value of 0.73 while MCMC has the lowest value of 0.67. Consequently, the interactions among the three different objectives resulted in a Pareto-optimal solution (Savic, 2002). The graphical comparison of the simulated runoff with observed runoff for the entire period of calibration and validation demonstrates a degree of representativeness and agreement with the observed runoff. However, for a sub-set period of calibration (1999–2000) and validation (2001–2002), there are some overestimations of the peak by some optimization techniques (e.g. MCMC) and the underestimation of the base flow by some other optimization techniques (e.g. SCE-R and DE) (Fig. 5). In contrast, MCMC represents the base flow well. The anomaly (Fig. 5) shows the deviations of the simulated run-off from the observed runoff. The highest deviation is seen in MCMC result while the lowest is seen in DE and SCE-R. However, the degree of anomaly seems to be lesser during the validation period. Furthermore, SCE-R, DE, PSO and MALS returned reasonable optimized objective functions for both calibration and validation periods (Table 4).

For the second episode of the calibration (1980–1995) (Table 4), the results show that SCE-R, DE, PSO and MALS provide the best parameters. They have the NSE, KGE and RMSE values of 0.89, 0.79 and 0.23 respectively. This agrees with Jain and Srinivasulu (2009) who stated that the genetic algorithms are efficient for hydrologic model calibration. LOMS and MCMC have lower NSE and KGE values. This same behaviour is exhibited during the validation period (1996–2011). In both cases, LOMS and MCMC have the lowest performance.

It is worthy to note that changing the calibration episodes has little to no effect on the generated model parameters. For example, in SCE-R method for both calibration episodes, X1 is between 100.25–101.78 mm, X2 is between −14.96 to −14.98 mm while X3, X4 and X5 do not change. For MALS, X1 does not change, X2 ranges from −14.95 to −14.96 mm, X3 is from 998.68–1000.14 mm while X4 and X5 do not change. The range of these similar calibration parameters during both episodes for the different optimization techniques shows the robustness of the calibration efficiencies of these methods. Furthermore, the applied calibration methods show reasonable abilities to simulate runoff with a satisfactory level of accuracy. Hence, multi-objective calibrations are of great advantage as it ensures desired outcomes in hydrological applications (Yapo et al., 1998; Efstratiadis and Koutsoyiannis, 2010; Mostafaie et al., 2018).

Additionally, Table 4 also shows that different parameters can produce a very similar objective function. For example, parameter X1 varies from 100.25 for SCE-R to 800.95 for MCMC, whereas parameter X3 varies from 1000.52 for SCE-R to 200.35 for MCMC. This is a compensating process leading to the well-known phenomena of equifinality, ambiguity, non-uniqueness and identifiability of parameters. Beven (2006) stated that during hydrological simulations, acceptable good fits are regularly located beyond the Pareto optima regions. This may be linked to the different parameterisation processes of hydrological systems as observed in the hydrological model (Poissant et al., 2017). Therefore, the uncertainties associated with the hydrological model's parameterisation processes do not permit a solitary or explicit mathematical solution to parameters identification problem (Beck, 1987; Beven, 2006). This is uncertainty in flow forecast. However, the issue of equifinality can be reduced by improving the parameterisation schemes of the model as well as the model structures and parameter values. Therefore, equifinality is this context is seen as finding multiple practical

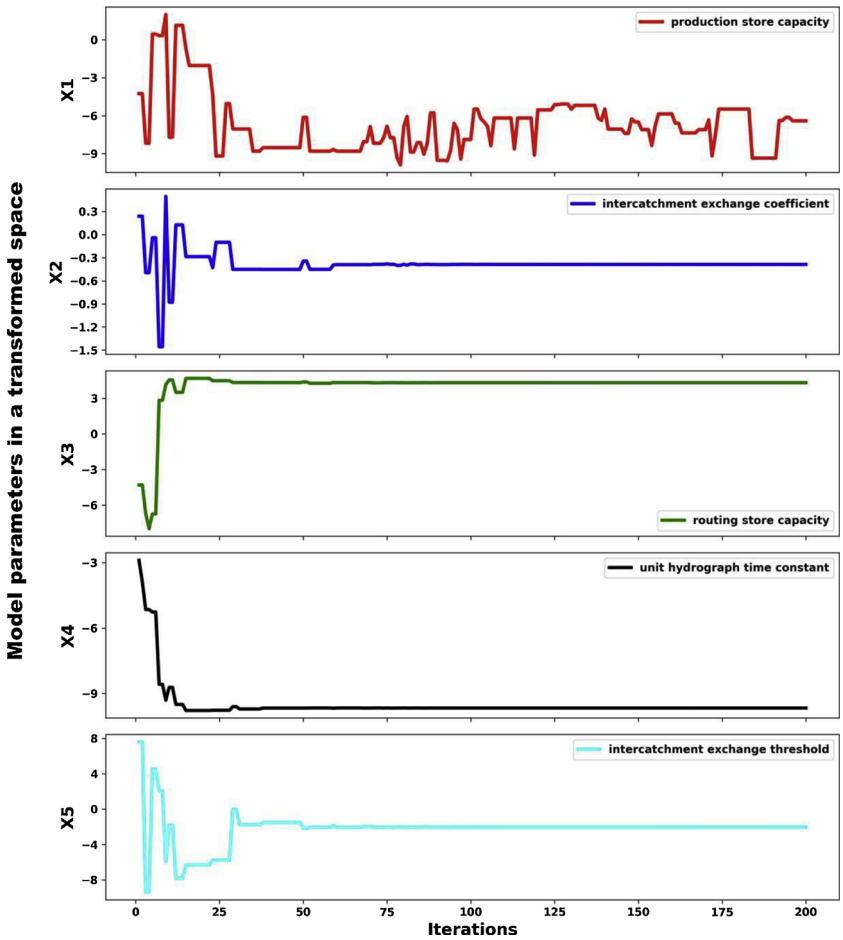

Fig. 6. Convergence of model parameters from the DE optimization method.

hypotheses about how the system works (Beven, 2002).

4.2. Convergence of model parameters

The assessment of the model parameters convergence shows the number of iterations needed for the model parameters to converge towards a good optimized solution.

To evaluate these convergences, the parameters are transformed into real space and analysed based on the trade-off between computational period and simulation accuracy. According to Madsen (2000, 2003), the parameter space limits are based on the model's physical and mathematical constraints, physical features of the system and simulation trials.

As an illustration, the convergence for model parameters generated from the DE optimization method is presented in Fig. 6. The result shows that X4 converges faster than the rest of the parameters. X4 converges at about 30 iterations while the slowest converging parameter is X1, which do not converge at 200 iterations. This means that it takes longer for every individual in the X1 population to be identical in order to reach an optimized solution. Hence, the computation time is prolonged. The results for other optimization methods are presented in the supplementary file.

4.3. Flow characteristics

In an attempt to further understand the hydrological properties of the basin as simulated by individual optimization methods, the statistics of the base flow and high flow spells is computed. The base flow separation method follows Ladson et al. (2013).

4.3.1. Baseflow

In Table 5, the base flow is generated for both calibration and validation periods for the two phases. For calibration period, SCE-R, DE, MALS and PSO clearly overestimate the mean daily base flow by 0.06 mm/day while LOMS and MCMC underestimate it by −0.07 mm/day. The overestimation by SCE-R, DE, PSO, MALS and the underestimation by LOMS and MCMC is seen to persist for the

Table 5
Base flow statistics.

Base Flow (mm/day)			
Strategy	Mean Daily Flow	Median Daily Flow	Mean Base flow Volume
Calibration (1974–2000)			
OBS	0.59	0.00	0.08
SCE-R	0.65	0.12	0.18
DE	0.65	0.12	0.18
PSO	0.65	0.12	0.18
MALS	0.65	0.12	0.18
LOMS	0.52	0.05	0.02
MCMC	0.52	0.04	0.02
Validation (2001–2013)			
OBS	0.68	0.00	0.09
SCE-R	0.74	0.13	0.20
DE	0.74	0.13	0.20
PSO	0.74	0.13	0.20
MALS	0.74	0.13	0.20
LOMS	0.63	0.04	0.05
MCMC	0.62	0.04	0.04

OBS means observation.

median daily base flow and mean base flow volume. For the validation period, SCE-R, DE, PSO and MALS continue to overestimate the base flow parameters while LOMS and MCMC continue with the underestimation.

4.3.2. High flow spells

The number of high flow spell events is underestimated by SCE-R, DE, PSO, MALS while LOMS and MCMC overestimate it for both calibration and validation period (Table 6). However, the highest overestimation is seen LOMS (112) during calibration and in MCMC (52) during validation. The same trend is repeated for the spell event frequency. LOMS and MCMC underestimate the maximum duration of high flow spell days during calibration by − -2 days while SCE-R, DE, PSO and MALS overestimate it by +13 days. During validation, all optimization methods underestimate this event by at least −11 days. The average annual maximum flows and flood skewness (the ratio of average annual maximum to mean daily flow) is overestimated by all methods during calibration and validation periods. The highest overestimation in flood skewness is by LOMS during the calibration period (12.43) and MCMC during the validation period (11.23). All calibration techniques fairly predict the correct average day of the year on which maximum flows occur during the calibration period with a degree of ± 2 days. However, LOMS and MCMC overestimate it by +5 days during the validation period.

Table 6
High flow spells statistics.

High flow spells							
Strategy	No of spell events	Spell event frequency (no/year)	Maximum duration of spell events (days)	average annual maximum flow (mm)	coefficient of variation of annual maximum flows	flood skewness	average day of the year on which maximum flows occur (day)
Calibration (1974–2000)							
OBS	91	3.37	77	6.19	27.60	10.43	229
SCE-R	72	2.67	90	7.02	32.57	10.88	228
DE	71	2.63	90	7.03	32.58	10.90	228
PSO	72	2.67	90	7.03	32.57	10.88	228
MALS	71	2.63	90	7.03	32.58	10.90	228
LOMS	112	4.15	68	6.48	26.60	12.43	231
MCMC	110	4.07	68	6.45	26.46	12.34	231
Validation (2001–2013)							
OBS	37	2.85	79	6.85	22.83	10.01	231
SCE-R	34	2.62	68	7.84	28.80	10.61	231
DE	34	2.62	68	7.84	28.80	10.61	231
PSO	34	2.62	68	7.84	28.78	10.61	231
MALS	34	2.62	68	7.84	28.80	10.61	231
LOMS	50	3.85	66	6.98	22.88	11.15	236
MCMC	52	4.00	66	7.00	22.82	11.23	236

Flood Skewness is the ratio of average annual maximum to mean daily flow.

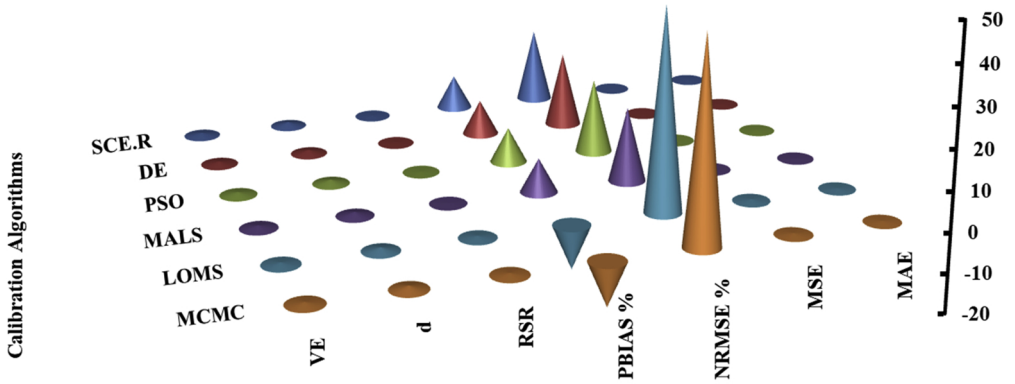

Performance metrics

	MAE	MSE	NRMSE %	PBIAS %	RSR	d	VE
SCE.R	0.16	0.05	18.4	8.4	0.18	0.99	0.74
DE	0.17	0.06	18.5	8.6	0.19	0.98	0.73
PSO	0.16	0.05	18.4	8.6	0.18	0.99	0.74
MALS	0.16	0.05	18.4	8.4	0.18	0.99	0.74
LOMS	0.27	0.39	50	-10.9	0.5	0.93	0.56
MCMC	0.28	0.4	50.1	-11	0.51	0.93	0.56

Fig. 7. Performance evaluation of each calibration algorithms between 1974 and 2013. MAE is the mean absolute error, MSE is the mean square error, NRMSE is the normalized root mean square error, PBIAS is the percentage of bias, RSR is the ratio of root mean square error to the standard deviation, d is the index of agreement and VE is the volumetric efficiency.

Generally, multi-objective calibration is seen to have reliable applications to multi-variable measurements and multi-response approaches to various hydrological processes (e.g. the low and peak flows) (Madsen, 2003; Mostafaie et al., 2018).

4.4. Performance metrics

The summary of the numerical performance metrics for each of the optimization technique implemented is shown in Fig. 7. The performance metric is for the entire calibration and validation period. The performance evaluation shows that MCMC has the highest values of mean absolute error (0.28) and mean square error (0.40) while LOMS and MCMC record a low volumetric efficiency of 0.56 (Fig. 7). This means that these two optimization techniques mismatch the fractional volume of water delivered per unit time. However, all other techniques perform better in the fraction of water delivered. When evaluated against different performance metrics, it is evident that several parameters returned equally good model outputs (Mostafaie et al., 2018).

4.5. Joint time-frequency signal

The wavelet spectra plot of the runoff variance across different time scales for the first simulation phase (1974–2013) shows slight differences in the results of the optimization techniques (Fig. 8). The wavelet coefficients estimates are only reliable in the areas within the cone of influence i.e. the solid black lines which represent the 95 % confidence level. For the observation (OBS), there is 3–4 years periodicity of high-frequency power from 1974 to 1992. However, this periodicity is only significant between 1979–1992 and 2005–2008. The highest wavelet power of between 11 and 12 years is captured by all techniques. This high periodicity is assumed to be caused by high rainfall variability as well as the impact of human activities in the runoff in the basin (Nicholson, 2001; Umar and Ankidawa, 2016; Adeyeri et al., 2018). Furthermore, the significant power between 1989 and 1997 in the OBS is underestimated by DE, PSO, MALS and LOMS methods. These phenomena are captured by different optimization techniques. Likewise, the span of significant powers varies from one method to the other. For example, MALS underestimated the span of powers while MCMC overestimated it. A dominant episode of significant power between 6 and 7 years is observed between 1990 and 2000. This is accurately replicated by the SCE-R while other techniques apart from MCMC underestimated it. Furthermore, the wavelet phases (blue arrows) are accurately captured by all techniques. Arrows pointing up (down) show a lead (lag) of 90° from the first time series to the second time series. If the time series move together, there is a zero-phase difference. If the arrows are pointing left (right), it means the time series are anti-phase (in-phase) i.e. negatively (positively) correlated. In general, the magnitude of the wavelet coefficient is accurately represented by all optimization techniques.

4.6. Implications for the KYB and the Lake Chad

The KYB is a sub-basin of the larger Lake Chad basin. It represents 35 % of the Lake Chad Basin. Its rivers contribute significantly

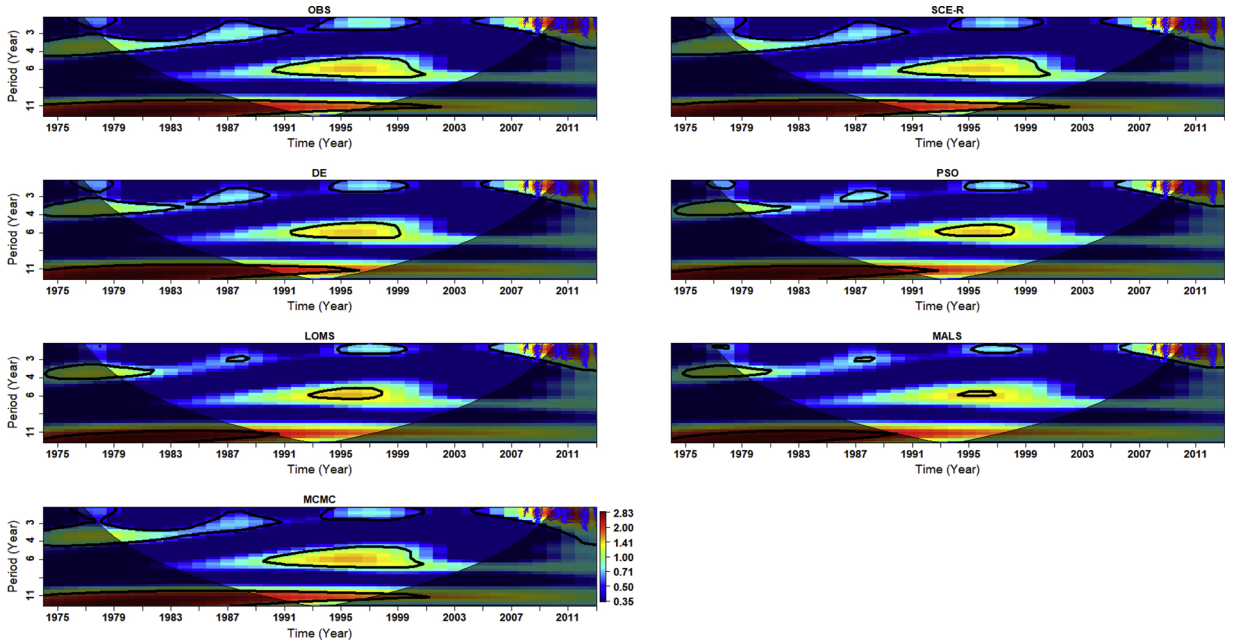

Fig. 8. Wavelet spectra plot for runoff generated by observation, the Differential Evolution (DE), the Local Optimization-Multi Start (LOMS), the Bayesian Markov Chain Monte Carlo (MCMC), the Shuffled Complex Evolution-Rosenbrock's function (SCE-R), the Multi-objective Particle the Swarm Optimization (PSO), and the Memetic Algorithm with Local Search Chains (MALS) optimization method between 1974 and 2013. Solid black line represents the 95 % confidence level.

to the Lake Chad. Therefore, the hydrology and ecosystem of the KYB particularly influence the drying or recovery of the Lake Chad. Over the past decades, the KYB had witnessed episodes of drought and rainfall recovery (Thompson and Polet, 2000; Adeyeri et al., 2019b). This had led to the modification of the hydrological regimes and systems. Since these systems are complex, there is a need for an accurate representation of the basin's hydrological features. On the representation of base flow, this maintains the water quality, river's biodiversity, productivity and aquatic species' migration by influencing the surface channel and the hyporheic zones (Malcolm et al., 2004). Thus, an accurate representation of the baseflow is important for making relevant decisions for sustainable biodiversity management, environmental policies, river restoration as well as functional aquatic ecosystem preservation (Hitchman et al., 2018). In the same vein, the high flow could potentially maintain the food chain balance by reviving the wetlands in the basin (Adeyeri et al., 2019a). This will also replenish Lake Chad. On the other hand, excess water from continuous high flow spell could cause flooding, consequently affecting properties, farm produce and farmlands. Hence, the water resource will be greatly stressed while the socio-economic activity will be hampered. According to Cook et al. (2015), the warming climate could aggravate the stress on freshwater resources. Hence, to accurately manage the freshwater resources, a proper representation of the hydrological system is essential, especially in the face of changing climate.

5. Summary and conclusion

Different multi-objective and multi-optimization techniques have been evaluated in this study for the GR5J hydrological model applied to the case of the Komadugu-Yobe basin KYB. The calibration process involved the use of six evolutionary optimization methods (SCE-R, DE, PSO, MALS, LOMS and MCMC) and three combined objective functions (i.e. minimizing RMSE, maximizing both NSE and KGE). The robustness of the calibration approaches was validated by considering two episodes (1974–2013 and 1980–2011) for the analysis.

The applied calibration methods showed reasonable abilities to simulate runoff with a satisfactory level of accuracy. The results of the flow statistics were not universally consistent as some optimization methods overestimate while others continually underestimate the flow representation. For example, MCMC underestimated the maximum duration of high flow spell by -2 days while MALS overestimated it by $+13$ days.

For the particular case of KYB, we found that the DE and the SCE-R methods performed best. The multi-objective computational assessment for each optimization methods to reach the optimal Pareto solutions showed that MALS exhibits the highest number of iterations while the PSO had the highest number of simulations for both calibration periods. The lowest iterations and simulations were exhibited by the SCE-R approach in all cases. Comparing the computational period and the performance metric of SCE-R indicates the trade-off balance between computational period and simulation accuracy.

Based on these evaluations, it is concluded that the combination of multi-objective functions and multi-optimization techniques for optimal Pareto sets for GR5J model parameters over the KYB do not only improve the stability of the model parameters during

calibration, but also improve the optimization ability of the calibration algorithms towards more accurate and robust representation of the river runoff in the basin. Furthermore, the auto-calibration method is more efficient as it circumvents the interference of anthropogenic factors as observed in manual calibrations (Madsen, 2000; Wu et al., 2017).

Future work should incorporate more methodologies to ascertaining the different sources of uncertainty in model parameters, model structure and input dataset as well as error structure and probabilities, especially during calibration.

Declaration of Competing Interest

None

Acknowledgement

The first author was supported by the doctoral scholarship from the Federal Ministry of Education and Research (BMBF) and West African Science Service Centre on Climate Change and Adapted Land Use (WASCAL).

Appendix A. Supplementary data

Supplementary material related to this article can be found, in the online version, at doi:https://doi.org/10.1016/j.ejrh.2019.100655.

References

Adeyeri, O.E., Lamptey, B.L., Lawin, A.E., Sanda, I., 2017. Spatio-temporal precipitation trend and homogeneity analysis in Komadugu-Yobe Basin, Lake Chad Region. J. Climatological Weather Forecasting 5, 214. https://doi.org/10.4172/2332-2594.1000214.

Adeyeri, O.E., Laux, P., Lawin, A.E., Arnault, J., 2018. Assessing the impact of human activities and rainfall variability on the river discharge of Komadugu-Yobe Basin, Lake Chad Area. J. Environ. Earth Sci (Submitted).

Adeyeri, O.E., Laux, P., Lawin, A.E., Ige, S.O., Kunstmann, H., 2019a. Analysis of hydrometeorological variables over the transboundary Komadugu-Yobe basin, West Africa. J. Water Clim. Chang. https://doi.org/10.2166/wcc.2019.283.

Adeyeri, O.E., Lawin, A.E., Laux, P., Ishola, K.A., Ige, S.O., 2019b. Analysis of climate extreme indices over the Komadugu-Yobe basin, Lake Chad region: past and future occurrences. Weather Clim. Extrem. https://doi.org/10.1016/j.wace.2019.100194.

Arnold, J.G., Fohrer, N., 2005. SWAT2000: current capabilities and research opportunities in applied watershed modelling. Hydrol. Process. 19 (3), 563–572.

Braak, C.J.T., 2006. A Markov Chain Monte Carlo version of the genetic algorithm differential evolution: easy Bayesian computing for real parameter spaces. Stat. Comput. 16, 239–249.

Barbara, C., Victor, V., Annemarie, L., Konrad, A., Ingeborg, A., Johanna, N., 2018. Intercomparison of methods to homogenize daily relative humidity. Int. J. Climatol. https://doi.org/10.1002/joc.5488.

Beck, M.B., 1987. Water quality modelling: a review of the analysis of uncertainty. Water Resour. Res. 23 (8), 1393–1442.

Bekele, E.G., Nicklow, J.W., 2007. Multi-objective automatic calibration of SWAT using NSGA-II. J. Hydrol. 341 (3), 165–176.

Bellin, A., Majone, B., Cainelli, O., Alberici, D., Villa, F., 2016. A continuous coupled hydrological and water resources management model. Environ. Model. Softw. 75, 176–192.

Bergmeir, C., Molina, D., Benítez, J.M., 2016. Memetic algorithms with local search chains in R: the Rmalschains package. J. Stat. Softw. 75 (4), 1–33.

Beven, K.J., 2011. Rainfall-runoff Modelling: the Primer. Wiley, New York.

Beven, K.J., 2006. A manifesto for the equifinality thesis. J. Hydrol. 320, 18–36.

Beven, K.J., 2002. Towards an alternative blueprint for a physically-based digitally simulated hydrologic response modelling system. Hydrol. Process. 16 (2), 186–206.

Clerc, M., Kennedy, J., 2002. The particle swarm-explosion, stability, and convergence in a multidimensional complex space. IEEE Trans. Evol. Comput. 6 (1), 58–73.

Cook, B.I., Ault, T.R., Smerdon, J.E., 2015. Unprecedented 21st-century drought risk in the American Southwest and Central Plains. Sci. Adv. 1, e1400082.

Cooper, V.A., Nguyen, V.T.V., Nicell, J.A., 2007. Calibration of conceptual rainfall-runoff models using global optimization methods with hydrologic process-based parameter constraints. J. Hydrol. 334 (3–4), 455–466.

Coron, L., Thirel, G., Delaigue, O., Perrin, C., Andréassian, V., 2017. The suite of lumped GR hydrological models in an r package. Environ. Model. Softw. 94, 166–171.

Criss, R.E., Winston, W.E., 2008. Do Nash values have value? Discussion and alternate proposals. Hydrol. Process. 22 (14), 2723–2725.

Deb, K., Pratap, A., Agarwal, S., Meyarivan, T.A., 2002. A fast and elitist multiobjective genetic algorithm: NSGA-II. IEEE Trans. Evol. Comput. 6 (2), 182–197.

Doll, P., Kaspar, F., Lehner, B., 2003. A global hydrological model for deriving water availability indicators: model tuning and validation. J. Hydrol. 270 (1–2), 105–134.

Domonkos, P., Coll, J., 2017. Homogenisation of temperature and precipitation time series with ACMANT3: method description and efficiency tests. Int. J. Climatol. 37, 1910–1921.

Donelly-Makowecki, L.M., Moore, R.D., 1999. Hierarchical testing of three rainfall-runoff models in small forested catchments. J. Hydrol. 219 (3–4), 136–152.

Duan, Q.Y., 2003. Global Optimization for Watershed Model Calibration. Calibration of Watershed Models. American Geophysical Union, Washington DC, pp. 89–104.

Duan, Q.Y., Gupta, V.K., Sorooshian, S., 1993. Shuffled complex evolution approach for effective and efficient global minimization. J. Optim. Theory Appl. 76 (3), 501–521.

Duan, Q.Y., Sorooshian, S., Gupta, V.K., 1992. Effective and efficient global optimization for conceptual rainfall-runoff models. Water Resour. Res. 28 (4), 1015–1031.

Dumedah, G., Berg, A.A., Wineberg, M., Collier, R., 2010. Selecting model parameter sets from a trade-off surface generated from the non-dominated sorting genetic algorithm-II. Water Resour. Manag. 24 (15), 4469–4489.

Efstratiadis, A., Koutsoyiannis, D., 2010. One decade of multi-objective calibration approaches in hydrological modelling: a review. Hydrol. Sci. J. 55 (1), 58–78.

Foglia, L., Hill, M.C., Mehl, S.W., Burlando, P., 2009. Sensitivity analysis, calibration, and testing of a distributed hydrological model using error-based weighting and one objective function. Water Resour. Res. 45 (6).

Gay, D., 1990. Usage Summary for Selected Optimization Routines. Computing Science Technical Report 153. AT&T Bell Laboratories, Murray Hill.

Goswami, M., Kieran, M.O., 2007. Comparative assessment of six automatic optimization techniques for calibration of a conceptual rainfall-runoff model. Hydrol. Sci. J. 52 (3), 432–449.

Gupta, H.V., Kling, H., Yilmaz, K.K., Martinez, G.F., 2009. Decomposition of the mean squared error and NSE performance criteria: implications for improving hydrological modelling. J. Hydrol. 377 (1–2), 80–91.

Gupta, H.V., Sorooshian, S., Hogue, T., Boyle, D., 2003. Advances in the automatic calibration of watershed models. Proceedings of American Geophysical Union on the Calibration of Watershed Models, Water Science and Application 9–28 6.

Gupta, H.V., Sorooshian, S., Yapo, P.O., 1998. Toward improved calibration of hydrologic models: multiple and noncommensurable measures of information. Water Resour. Res. 34 (4), 751–763.

Haario, H., Laine, M., Mira, A., Saksman, E., 2006. DRAM: efficient adaptive MCMC. Stat. Comput. 16 (4), 339–354.

Haario, H., Saksman, E., Tamminen, J., 2005. Componentwise adaptation for high dimensional MCMC. Comput. Stat. 20 (2), 265–274.

Hitchman, S.M., Mather, M.E., Smith, J.M., Fencl, J.S., 2018. Identifying keystone habitats with a mosaic approach can improve biodiversity conservation in disturbed ecosystems. Glob. Chang. Biol. 24, 308–321.
Ilonen, J., Kamarainen, J.K., Lampinen, J., 2003. Differential evolution training algorithm for feed-forward neural networks. Neural Process Letters 7 (1), 93–105.
Jain, A., Srinivasulu, S., 2009. Hydrologic model calibration using evolutionary optimisation. In: Abrahart, R.J., See, L.M., Solomatine, D.P. (Eds.), Practical Hydroinformatics. Water Science and Technology Library, v68. Springer, Berlin, Heidelberg.
Joshi, R., Sanderson, A.C., 1999. Minimal representation multisensory fusion using differential evolution. IEEE Trans. Syst. Man Cybern. A. Syst. Hum. 29 (1), 63–76.
Kennedy, J., Eberhart, R.C., 1995. Particle swarm optimization. Proceedings of IEEE International Conference on Neural Networks 1942–1948 4.
Kling, H., Fuchs, M., Paulin, M., 2012. Runoff conditions in the upper Danube basin under an ensemble of climate change scenarios. J. Hydrol. 424–425, 264–277.
Kumar, R., Samaniego, L., Attinger, S., 2013. Implications of distributed hydrologic model parameterization on water fluxes at multiple scales and locations. Water Resour. Res. 49.
Ladson, A.R., Brown, R., Neal, B., Nathan, R., 2013. A standard approach to baseflow separation using the Lyne and Hollick filter. Aust. J. Water Resour. 17 (1) 173–18.
Lampert, D.J., Wu, M., 2015. Development of an open-source software package for watershed modelling with the Hydrological Simulation Program in FORTRAN. Environ. Model. Softw. 68, 166–174.
Lavenne, A., Thirel, G., Andréassian, V., Perrin, C., Ramos, M., 2016. Spatial variability of the parameters of a semi-distributed hydrological model. Proceedings of IAHS 373. pp. 87–94.
Legates, D.R., McCabe, G.J., 1999. Evaluating the use of "Goodness-of-Fit" measures in hydrologic and hydroclimatic model validation. Water Resource Research 35, 233–241.
Le Moine, N., 2008. Le Bassin Versant De Surface Vu Par Le Souterrain: Une Voie d'amélioration Des Performances Et Du Réalisme Des Modèles Pluie-débit? Dissertation. Université Pierre et Marie Curie, Paris, France.
Li, J., Heap, A.D., 2014. Spatial interpolation methods applied in the environmental sciences: a review. Environ. Model. Softw. 53, 173–189.
Li, X., Weller, D.E., Jordan, T.E., 2010. Watershed model calibration using multi-objective optimization and multi-site averaging. J. Hydrol. 380 (3), 277–288.
Lindstrom, G., Pers, C., Rosberg, J., Stromqvist, J., Arheimer, B., 2010. Development and testing of the HYPE (Hydrological Predictions for the Environment) water quality model for different spatial scales. Hydrol. Res. 41 (3–4), 295–319.
Lu, D., Ye, M., Meyer, P.D., Curtis, G.P., Shi, X., Niu, X.F., Yabusaki, S.B., 2013. Effects of error covariance structure on the estimation of model averaging weights and predictive performance. Water Resour. Res. 49 (9), 6029–6047.
Madsen, H., 2003. Parameter estimation in distributed hydrological catchment modeling using automatic calibration with multiple objectives. Adv. Water Resour. 26 (2), 205–216.
Madsen, H., 2000. Automatic calibration of a conceptual rainfall-runoff model using multiple objectives. J. Hydrol. 235 (3), 276–288.
Malcolm, I.A., Soulsby, C., Youngson, A.F., Hannah, D.M., Mclaren, I.S., Thorne, A., 2004. Hydrological influences on hyporheic water quality: implications for salmon egg survival. Hydrol. Process. 18, 1543–1560.
Mathevet, T., Michel, C., Andreassian, V., Perrin, C., et al., 2006. A bounded version of the Nash-Sutcliffe criterion for better model assessment on large sets of basins. In: In: Andréassian (Ed.), Large Sample Basin Experiments for Hydrological Model Parameterization: Results of the Model Parameter EXperiment [Online], vol. 307. International Association of Hydrological Sciences, IAHS Publications, Wallingford, pp. 211–219.
Molina, D., Lozano, García-Martínez, M., Herrera, C.F., 2010. Memetic algorithms for continuous optimisation based on local search chains. Evol. Comput. 18 (1), 27–63.
Moriasi, D.N., Arnold, J.G., Van Liew, M.W., Bingner, R.L., Harmel, R.D., Veith, T.L., 2007. Model evaluation guidelines for systematic quantification of accuracy in watershed simulations. Trans. Asabe 50, 885–900.
Mostafaie, A.E., Forootan, E.A., Safari, A., Schumacher, M., 2018. Comparing multi-objective optimization techniques to calibrate a conceptual hydrological model using in situ runoff ; and daily GRACE data. Comput. Geosci. 22, 789–814.
Narasayya, K., Roman, U.C., Meena, B.L., Sreekanth, S., Naveed, A.S., 2013. Prediction of storm-runoff using physically-based hydrological model for burhanpur watersheds, India. Int. J. Remote Sens. Geosci. 2, 76–85.
Nash, J.E., Sutcliffe, J.V., 1970. River flow forecasting through conceptual models part 1. A discussion of principles. J. Hydrol. 10 (3), 282–290.
Nicholson, S.E., 2001. Climatic and environmental change in Africa during the last two centuries. Clim. Chang. Res. Lett. 17, 123–144.
Ning, S., Ishidaira, H., Wang, J., 2015. Calibrating a hydrological model by a step-wise method using GRACE TWS and discharge data. Hydraul. Eng. J. 71 (4), 85–90.
Oudin, L., Michel, C., Anctil, F., 2005. Which potential evapotranspiration input for a lumped rainfall-runoff model? J. Hydrol. 303 (1–4), 275–289.
Perrin, C., Michel, C., Andreassian, V., 2003. Improvement of a parsimonious model for streamflow simulation. J. Hydrol. 279 (1), 275–289.
Poissant, D., Arsenault, R., Brissette, F., 2017. Impact of parameter set dimensionality and calibration procedures on streamflow prediction at ungauged catchments. J. Hydrol. Reg. Stud. 12, 220–237.
Qin, H., Zhou, J., Lu, Y., Li, Y., Zhang, Y., 2010. Multi-objective cultured differential evolution for generating optimal trade-offs in reservoir flood control operation. Water Resour. Manag. 24 (11), 2611–2632.
Rakovec, O., Kumar, R., Attinger, S., Samaniego, L., 2016. Improving the realism of hydrologic model functioning through multivariate parameter estimation. Water Resour. Res. 52, 7779–7792.
Riquelme, N., Von Lucken, C., Baran, B., 2015. Performance metrics in multi-objective optimization. In: Computing Conference (CLEI), 2015 IEEE. Latin American. pp. 1–11.
Sahoo, D., Smith, P.K., Ines, A.V.M., 2010. Autocalibration of HSPF for simulation of streamflow using a genetic algorithm. Trans. Asabe 53, 75–86.
Savic, D., 2002. Single-objective vs. multiobjective optimisation for integrated decision support. Proceedings of the First Biennial Meeting of the International Environmental Modelling and Software Society 7–12.
Seong, C., Her, Y., Benham, B.L., 2015. Automatic Calibration Tool for Hydrologic Simulation Program-FORTRAN Using a Shuffled Complex Evolution Algorithm Water, vol. 7. pp. 503–527.
Singh, V.P., Woolhiser, D.A., 2002. Mathematical modelling of watershed hydrology. J. Hydrol. Eng. 7 (4), 270–292.
Sorooshian, S., Gupta, V.K., 1995. In: Singh, V.P. (Ed.), Model Calibration, Chapter 2 in Computer Models of Watershed Hydrology. Water Resources Publications Highlands Ranch, Littleton, pp. 23–68.
Storn, R., 1996. On the usage of differential evolution for function optimization. In: Proceedings of Biennial Conference of North America Fuzzy Information Processing Society. Berkeley, CA. pp. 519–523.
Storn, R., Price, K.V., 1997. Differential evolution-A simple and efficient heuristic for global optimization over continuous Spaces. J. Glob. Optim. 11, 341–359.
Thompson, J., Polet, G., 2000. Hydrology and land use in a Sahelian floodplain wetland. Wetlands 20, 636–659.
Umar, A.S., Ankidawa, B.A., 2016. Climate variability and basin management: a threat to and from wetlands of Komadugu Yobe Basin, North Eastern Nigeria. Asian J Eng Tech 4 (2), 25–36.
Valéry, A., Andréassian, V., Perrin, C., 2014. As simple as possible but not simpler: what is useful in a temperature-based snow-accounting routine? Part 2 -Sensitivity analysis of the Cemaneige snow accounting routine on 380 catchments. J. Hydrol. 517, 1176–1187.
Van Werkhoven, K., Wagener, T., Reed, P., Tang, Y., 2009. Sensitivity guided reduction of parametric dimensionality for multi-objective calibration of watershed models. Adv. Water Resour. 32 (8), 1154–1169.
Veleda, D., Montagne, R., Araujo, M., 2012. Cross-wavelet bias corrected by normalizing scales. J. Atmos. Oceanic Technol. 29, 1401–1408.
Wagener, T., 2003. Evaluation of catchment models. Hydrol. Process. 17 (16), 3375–3378.
Werth, S., Guntner, A., Petrovic, S., Schmidt, R., 2009. Integration of GRACE mass variations into a global hydrological model. Earth Planet Sci. Letters 277 (1), 166–173.
Wu, Q., Lui, S., Cai, Y., Li, X., Jiang, Y., 2017. Improvement of hydrological model calibration by selecting multiple parameter ranges. Hydrol. Earth Syst. Sci. 21, 393–407.
Xie, H., Longuevergne, L., Ringler, C., Scanlon, B.R., 2012. Calibration and evaluation of a semi-distributed watershed model of Sub-Saharan Africa using GRACE data. Hydrol. Earth Syst. Sci. 16 (9), 3083–3099.
Yapo, P.O., Gupta, H.V., Sorooshian, S., 1998. Multi-objective global optimization for hydrologic models. J. Hydrol. 204 (1), 83–97.
Yapo, P.O., Gupta, H.V., Sorooshian, S., 1996. Automatic calibration of conceptual rainfall-runoff models: sensitivity to calibration data. J. Hydrol. 181, 23–48.